Studia Geotechnica et Mechanica, Vol. XXX, No. 1–2, 2008

MULTI-SCALE MODELLING OF THE MECHANICAL BEHAVIOUR OF GROUTED SAND

PIERRE-YVES HICHER, CHRISTOPHE DANO

Research Institute of Civil and Mechanical Engineering, UMR CNRS, Ecole Centrale Nantes, Université de Nantes, Nantes, France.

CHING S. CHANG

Department of Civil Engineering, University of Massachusetts, Amherst, USA,
pierre-yves.hicher@ec-nantes.fr

Abstract: Such mechanical properties of sand as its stiffness, cohesion and, to a less extent, friction angle can be increased through the process of grouting. A constitutive model adapted for cohesive-frictional materials from a homogenization technique, which allowed us to integrate constitutive relations on the grain level, has been developed to obtain constitutive equations for the equivalent continuous granular medium. The local behaviour was assumed to obey Hertz–Mindlin's elastic law and Mohr–Coulomb's plastic law. The influence of the cement grout was modelled by means of adhesive forces between grains in contact. The intensity of these adhesive forces is the function of nature and the amount of grout present inside the material and can be reduced due to a damage mechanism at the grain contact during loading. In this paper, we present several examples of simulation which show that the model can reproduce with sufficient accuracy the mechanical improvement induced by grouting as well as the damage of the grain cementation during loading.

1. INTRODUCTION

The construction of underground structures on soft ground often requires the soil to be improved in order to ensure the safety and the stability of surrounding buildings. Grout permeation is an efficient technique for reducing permeability and for increasing stiffness and strength of coarse-to-medium grained soils with low initial mechanical properties. Since traditional organic grouts, such as silicate gels, have proved to be hazardous for groundwater, they have been prohibited over the years. New grouts, therefore, such as very fine cement suspensions and mineral grouts, have been developed for about the past twenty years (ZEBOVITZ et al. [17], BENHAMOU [3]). These new grouts present similar groutability performance as do previous chemical solutions. Their considerable advantage is that they prove to be stable with time. We can therefore take into account their improved mechanical properties in design. Experimental studies have shown that cementation in sands, including grouted sands, influences their mechanical properties by adding cohesion and tensile strength, increasing stiffness, without changing significantly the friction angle (AIREY [1], CLOUGH and SITAR [9], DANO [10], DANO et al. [12]).

Microstructural models for inelastic stress–strain behaviour of granular material can be derived from the properties of interparticle contacts. Considering the mean behaviour of all contacts in each orientation, the overall stress–strain behaviour can be obtained as an average of the contact behaviour for all orientations. The basic idea is to view the packing as represented by a set of microsystems. The inelastic behaviour of each microsystem is characterized and the overall stress–strain relationship of the packing is obtained from an average of the behaviours of microsystems. Along these lines, we have developed a new stress–strain model considering interparticle forces and displacements (CHANG and HICHER [6]). We have included in the model internal forces at the grain contacts in order to reproduce the effect of grain adhesion. In this paper, the adhesive forces are simulating the effects of a cement grout incorporated in the pores of the granular material.

2. MICROSTRUCTURAL MODEL

In this model, we envisage a granular material as a collection of contact particles. The deformation of a representative volume of the material is generated by the mobilization of contact particles in all orientations. Thus, the stress–strain relationship can be derived as an average of the mobilization behaviour of local contact planes in all orientations. For contact planes in the α^{th} orientation, the local forces f_i^α and the local movements δ_i^α can be denoted as follows: $f_i^\alpha = \{f_n^\alpha, f_s^\alpha, f_t^\alpha\}$ and $\delta_i^\alpha = \{\delta_n^\alpha, \delta_s^\alpha, \delta_t^\alpha\}$, where the subscripts *n*, *s*, and *t* represent the components in the three directions of the local coordinate system. The direction normal to the plane is denoted as *n*; the other two orthogonal directions, *s* and *t*, are tangential to the plane.

2.1. INTERPARTICLE BEHAVIOUR

2.1.1. ELASTIC PART

The contact stiffness of an orientation includes normal stiffness k_n^α and shear stiffness k_r^α of the contact plane. The elastic stiffness tensor is defined by

$$f_i^\alpha = k_{ij}^{\alpha e} \delta_j^{\alpha e}, \tag{1}$$

which can be related to the contact normal and shear stiffness:

$$k_{ij}^{\alpha e} = k_n^\alpha n_i^\alpha n_j^\alpha + k_r^\alpha (s_i^\alpha s_j^\alpha + t_i^\alpha t_j^\alpha). \tag{2}$$

The value of the stiffness for two elastic spheres can be estimated from Hertz–Mindlin's formulation (MINDLIN [16]). For sand grains, a revised form can be adopted, given by

$$k_n = k_{n0}\left(\frac{f_n}{G_g l^2}\right)^n; \quad k_t = k_{t0}\left(\frac{f_n}{G_g l^2}\right)^n, \tag{3}$$

where G_g is the elastic modulus for the grains, f_n is the contact force in normal direction. l is the branch length between the two particles. k_{n0}, k_{t0} and n are material constants.

2.1.2. PLASTIC PART

The elastic behaviour does not have a coupling effect (i.e., there is no shear induced by normal movements). However, plastic sliding does not necessarily occur along the tangential direction of the contact plane. The sliding direction may be upward or downward, and the shear dilation/contraction take place simultaneously. The dilatancy effect can be described by

$$\frac{d\delta_n^p}{d\Delta^p} = \frac{T}{f_n} - \tan\phi_0, \tag{4}$$

where ϕ_0 is a material constant which, in most cases, can be considered equal to the internal friction angle ϕ_μ. This equation can be derived by equating the dissipation work due to plastic movements to the friction loss of contact planes in the same orientation. Note that the generalized shear force T and the rate of plastic sliding $d\Delta^p$ can be defined as:

$$T = \sqrt{f_s^2 + f_t^2} \quad \text{and} \quad d\Delta^p = \sqrt{(d\delta_s^p)^2 + (d\delta_t^p)^2}. \tag{5}$$

The yield function is assumed to be of Mohr–Coulomb's type;

$$F(f_i, \kappa) = T - f_n \kappa(\Delta^p) = 0, \tag{6}$$

where $\kappa(\Delta^p)$ is an isotropic hardening/softening parameter. $F > 0$ indicates loading, otherwise unloading. The hardening function is defined by a hyperbolic curve in $\kappa - \Delta^p$ plane, which involves two material constants: ϕ_p and k_{p0}.

$$\kappa = \frac{k_{p0}\tan\phi_p \Delta^p}{|f_n|\tan\phi_p + k_{p0}\Delta^p}. \tag{7}$$

2.1.3. INTERLOCKING INFLUENCE

An important factor in granular modelling is the critical state concept. Under critical state, the granular material will remain at constant volume while it is subjected to a continuous distortion. The void ratio corresponding to this state is e_c.

The critical void ratio e_c is a function of mean stress. The relationship has traditionally been written as follows:

$$e_c = \Gamma - \lambda \log(p') \quad \text{or} \quad e_c = e_{\text{ref}} - \lambda \log\left(\frac{p'}{p_{\text{ref}}}\right), \tag{8}$$

Γ and λ are two material constants, p' is the mean stress of the packing, and (e_{ref}, p_{ref}) is a reference point on the critical state line.

The internal friction angle ϕ_μ is a constant for the material. However, the peak friction angle ϕ_p on a contact plane depends on the degree of interlocking by neighbouring particles, which can be related to the state of packing void ratio e by:

$$\tan\phi_p = \left(\frac{e_c}{e}\right)^m \tan\phi_\mu, \tag{9}$$

where m is a material constant (BIAREZ and HICHER [4]).

For dense packing, the peak frictional angle ϕ_p is greater than ϕ_μ. When the packing structure dilates, the degree of interlocking and the peak frictional angle are reduced, which results in a strain-softening phenomenon.

2.2. STRESS–STRAIN RELATIONSHIP

The stress–strain relationship for an assembly can be determined from integrating the behaviour of interparticle contacts in all orientations. In the integration process, a micro–macro relationship is required. Using the static hypotheses, we obtain the relation between the global strain and interparticle displacement (LIAO et al. [14]):

$$\dot{u}_{j,i} = A_{ik}^{-1} \sum_{\alpha=1}^{N} \dot{\delta}_j^\alpha l_k^\alpha, \tag{10}$$

where the branch vector l_k^α is defined as the vector joining the centres of two particles, and the fabric tensor is defined by

$$A_{ik} \sum_{\alpha=1}^{N} l_i^\alpha l_k^\alpha. \tag{11}$$

It is noted that in equation (10), the summation is not limited to direct contacts. The summation should also include indirect contacts of neighbouring particles within a Voronoi polygon. The mean force and moment on the contact plane of each orientation are

$$\dot{f}_j^{\alpha} = \dot{\sigma}_{ij} A_{ik}^{-1} l_k^{\alpha} V. \tag{12}$$

Using equation (3), it can be proved that the following relationships take place

$$\dot{\sigma}_{ij} = \frac{1}{V} \sum_{\alpha=1}^{N} \dot{f}_j^{\alpha} l_i^{\alpha} . \tag{13}$$

To discretise the orientation distribution into a finite number of orientations, the locations of integration points in a spherical coordinates are used. Each orientation has a weighting factor. We found that the results are more accurate by using a set of fully symmetric integration points. From a study of the performance of different numbers of orientations, we found an integration points of 74 to be adequate (CHANG and HICHER [6]).

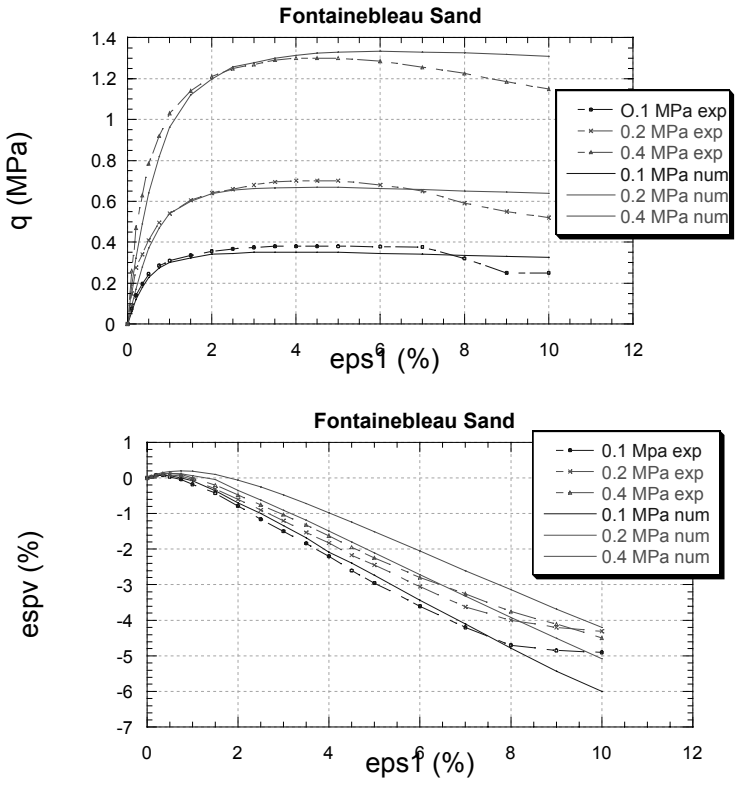

Fig. 1. Numerical simulations of triaxial tests of Fontainebleau Sand

Figure 1 presents the results of numerical simulations on Fontainebleau Sand ($I_D = 0.9$) subjected to triaxial tests at three different confining stresses (DANO [10]). Numerical simulations were performed using the set of material parameters summarized in table 1.

Table 1

Material parameters for Fontainebleau Sand

e_{ref}	p_{ref} (kPa)	λ	ϕ_μ (°)	ϕ_0 (°)	m
0.95	10	0.03	33	29	0.5

2.3. INTERNAL ADHESIVE FORCES

In order to take into account the effect of cement grout in the pores of the granular material, adhesive forces are added at each contact. The amplitude of those forces depends on the nature of the grout and on the concentration of the grout in cement particles. An extensive experimental work performed by DANO [10] showed the influence of these two parameters on the response of the grouted sand. The presence of adhesive forces on each contact plane affects the elastic properties given by equation (4). Effects of adhesive forces on the contact normal stiffness have been studied by CHANG and MISRA [5]. A simplified form of the stiffness considering adhesive force can be written as follows:

$$k_n = k_{n0}\left(\frac{f_n^*}{G_g l^2}\right)^n \tag{14}$$

with

$$f_n^* = f_n + \xi f_{ad}\,, \tag{15}$$

where ξ represents the relative influence of the adhesive force, function of the surface area of two neighbouring particles coated with the grout. ξ increases with the degree of cementation. At low degrees of cementation, the bond area is relatively small as the cement coats the particles to form weak bonds between two neighbouring particles. With the addition of cement, the bond area increases and the bonds become stronger, contributing to a higher stiffness of the grouted sand. The evolution of the shear modulus during a triaxial loading on a grouted specimen was measured using bender elements technique (DANO et al. [11]). After an initial phase of constant stiffness, the results showed a continuous decrease of the shear modulus, which was analysed as a damage of the bonded contacts (figure 5). Therefore, a damage law was introduced in the expression of the adhesive force amplitude, expressed as follows:

$$f_{\mathrm{ad}} = f_{\mathrm{ad}}^{0} \mathrm{e}^{-\eta_b(\rho-\sigma_b)} \quad \text{for} \quad \rho > \delta_b \,, \tag{16}$$

f_{ad}^{0} being the initial adhesive force, and η_b the factor of damage. ρ is an equivalent local displacement expressed by:

$$\rho[(\beta\delta_n^t)^2 + \Delta^2]^{1/2} \,, \tag{17}$$

where δ_n^t corresponds to the normal displacement in elongation. The value of δ_n^t is otherwise considered equal to zero. This hypothesis concerning the influence of the normal displacement in the damage law is linked with the fact that the tensile strength of the grout is only a small fraction of its compressive strength, which indicates that the rate of damage is much more important in traction than in compression, as in all cementitious materials (DANO et al. [12]).

The parameter β represents the relative influence of the normal displacement on the tangential displacement in the damage law. Usually, high values of β (>10) are selected due to a much greater influence of the tensile displacement compared to the tangential displacement on the grout damage.

δ_b corresponds to the limit value of ρ, under which no damage takes place (initial phase of constant stiffness).

Therefore, each contact produces a cohesive-frictional behaviour. During loading progressive damage of the cementitious bond leads to a decrease of adhesive forces, while the frictional shear resistance is progressively mobilized.

3. NUMERICAL SIMULATIONS OF TRIAXIAL TESTS ON GROUTED SANDS

In figures 2 and 3, we present two examples of Fontainebleau Sand (I_d = 0.95) samples reinforced with cement grout Intra-J at two different concentrations *C/W* = 0.17 and 0.23. The influence of the cement content in the sand pores can be seen by the increase of the material strength with the increase of *C/W* at every confining stress. The macroscopic cohesion *c* due to cemented intergranular bonds and the friction angle φ due to interparticle frictional contacts are determined by plotting the maximum strength envelope in Mohr–Coulomb's diagram. For uncemented granular soils, one obtains a straight-line failure envelope with zero cohesion. For grouted sands, a straight-line failure envelope that is almost parallel to that of the uncemented granular soil is obtained. In other words, the value of the friction angle is approximately the same, probably since permeation grouting with low injection pressures does not cause any disturbance of the particle assembly.

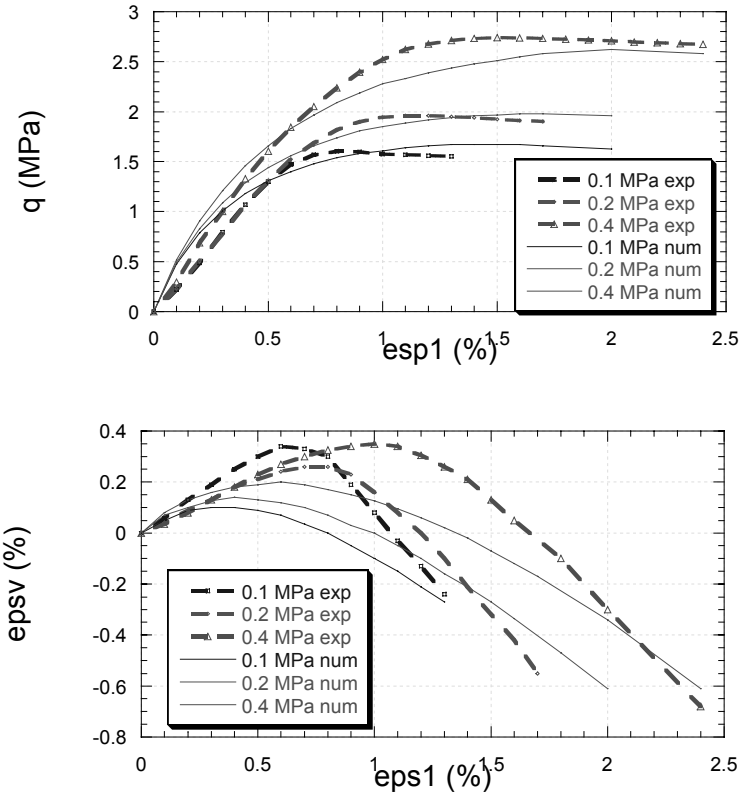

Fig. 2. Grouted Fontainebleau Sand by Intra-J $C/W = 0.175$

Numerical simulations were performed with the set of elastoplastic parameters determined in table 1 for non-cemented Fontainebleau Sand. The additional five parameters for the grout behaviour were determined from the stiffness decay curves. They are presented in tables 2 and 3. A comparison with experimental results in figures 2 and 3 shows that the model is capable of reproducing with sufficient accuracy the mechanical behaviour of grouted Fontainebleau Sand. The difference in initial stiffness between experimental and numerical results is mainly due to the compliance of the loading frame which induced higher measured axial displacement. Its influence can also be seen at the beginning of the ε_1–ε_v curves.

Table 2

Material parameters for Intra-J grout $C/W = 0.175$

f_{ad}^0	ξ	η_b	δ_b	β
0.01	20	0.003	0.0001	40

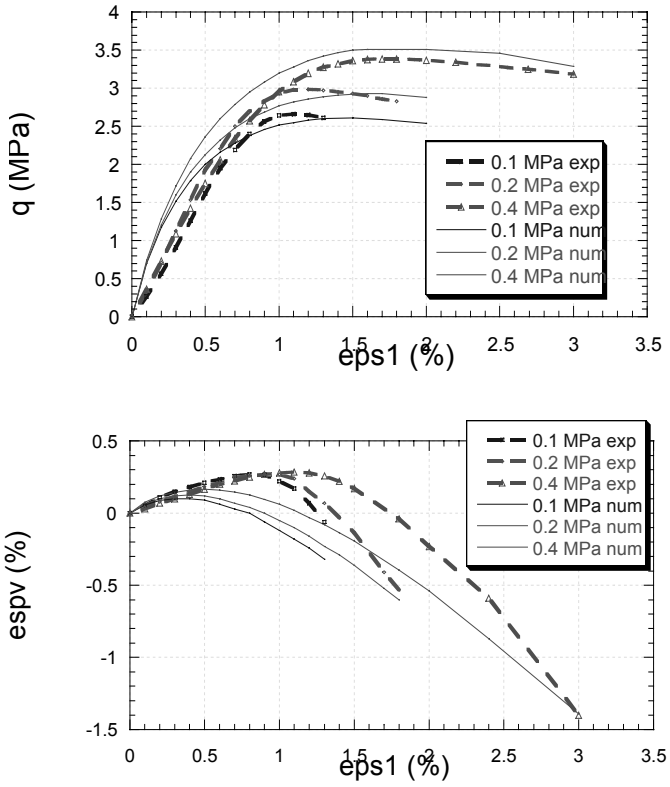

Fig. 3. Grouted Fontainebleau Sand by Intra-J $C/W = 0.23$

Table 3

Material parameters for Intra-J grout $C/W = 0.23$

f_{ad}^0	ξ	η_b	δ_b	β
0.015	25	0.003	0.0001	40

4. INFLUENCE OF CEMENT CONTENT

MAALEJ [15] studied the microstructure of the material using scanning electron microscope and mercury porosimeter. He was able to quantify very precisely the amount of cement grout inside the sand pores after injection. For a given cement grout at a given concentration *C/W*, this amount can vary during the grouting process due to the filtration of cement particles inside the sand pores. As a consequence, the concentration of the cement particles is higher near the point of injection and decreases with the distance from the injection point.

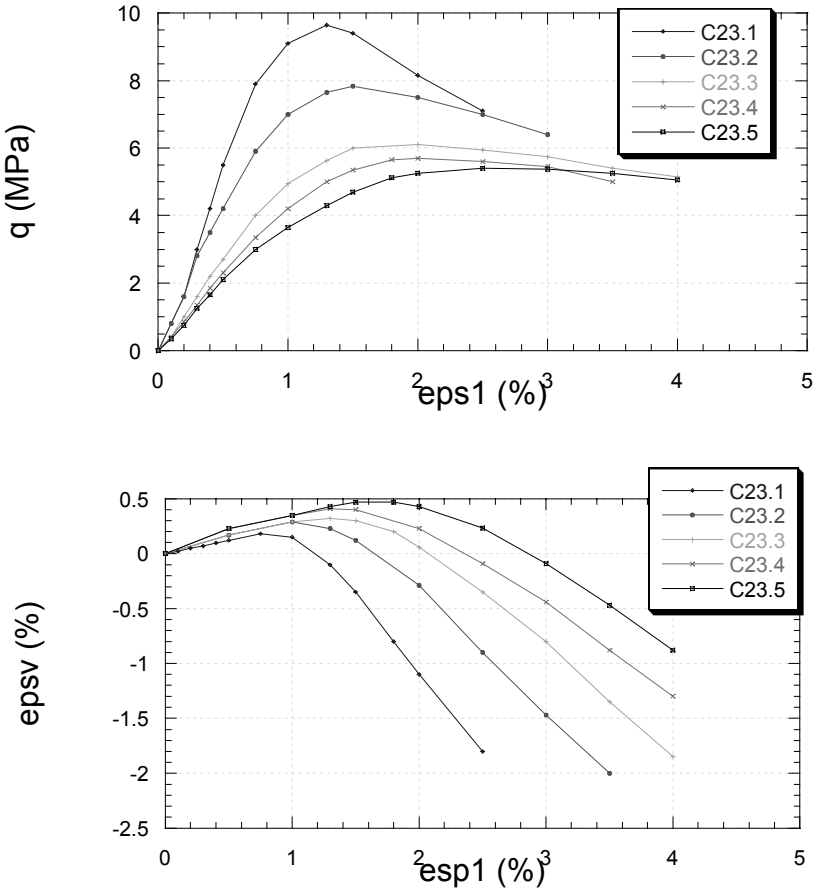

Fig. 4. Grouted Fontainebleau Sand. Experimental results for different grout concentrations

Figures 4 and 5 present experimental results and numerical simulations, respectively, for grouted Fontainebleau Sand specimens with different cement contents under a confining pressure equal to 0.8 MPa. The volumetric cement concentration varied from 0.22 in specimen 1 to 0.075 in specimen 5. The adhesive forces could be correlated to the cement content using a single linear relation:

$$f_{\mathrm{ad}}^{0} = 0.15\zeta \quad (f \text{ in } N), \tag{18}$$

ζ being the volumetric cement concentration (if e_0 is the initial sand void ratio and e_f the void ratio after grouting, $\zeta = e_0 - e_f$).

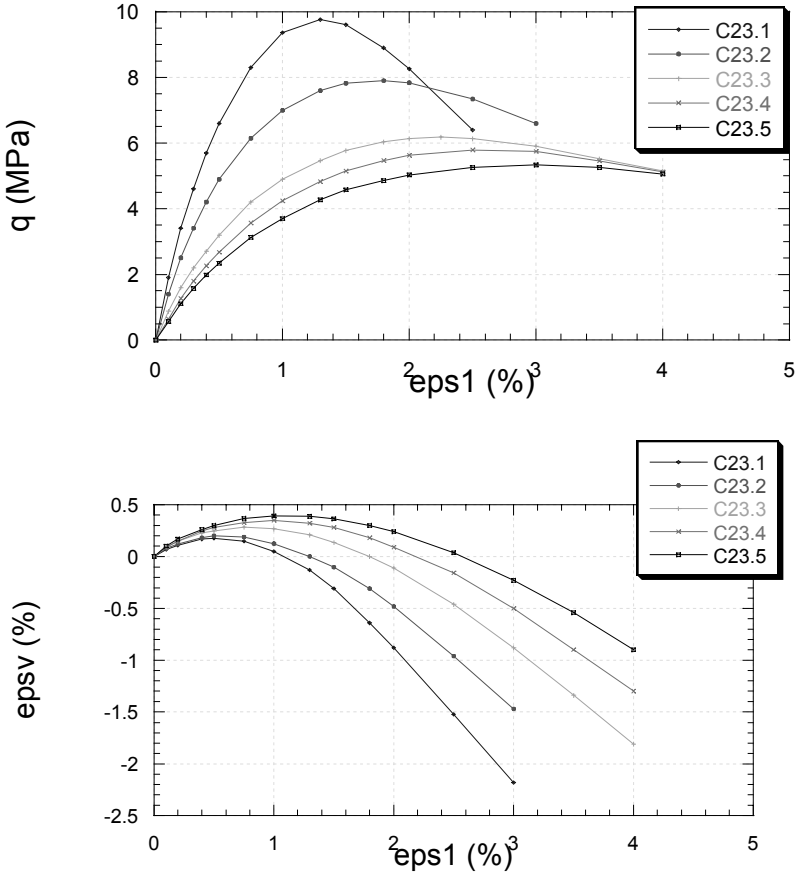

Fig. 5. Grouted Fontainebleau Sand. Numerical results for different grout concentrations

This linear relation is in agreement with the results presented by MAALEJ [15], who has showed that a linear relation could be found between the macroscopic cohesion c and the cement content ζ. It is therefore possible to predict the mechanical properties of an in situ grouted sand by taking into account the filtration process around the point of injection (see numerical simulations of grout propagation with filtration condition in CHUPIN et al. [7], [8]).

5. CONCLUSION

The microstructural approach is attractive conceptually, because it dispenses in having to deal with relations between the stress and strain tensors. Rather, we need to describe only a simple relation between the vectors of forces and relative displace-

ments on a contact plane, which thus requires fewer material parameters. The introduction of the grouting influence was made by means of an adhesive force, function of the nature and concentration of the cement grout. We demonstrated the ability of this new version of the model to reproduce the main features of grouted Fontainebleau sand with various cement grout concentrations.

REFERENCES

[1] AIREY D.W., *Triaxial testing of naturally cemented carbonate soil*, Journal of Geotechnical Engineering, 1993, 119(9), 1379–1398.

[2] BAIG S., PICORNELL M., NAZARIAN S., *Low strain shear moduli of cemented sands*, Journal of Geotechnical and Geoenvironmental Engineering, ASCE, 1997, 123(6), 540–545.

[3] BENHAMOU O., *Comportement rhéologique des coulis de liants hydrauliques ultrafins destinés à l'injection*, PhD thesis, Ecole de Géologie de l'Ingénieur, Ecole Nationale Supérieure des Mines de Paris, 1994 (in French).

[4] BIAREZ J., HICHER P.-Y., *Elementary Mechanics of Soil Behaviour*, Balkema, 1994, p. 208.

[5] CHANG C., MISRA A., *Micromechanical modelling of cemented sands under low amplitude oscillations*, Geotechnique, 1990, 40, (2), 251–263.

[6] CHANG C.S., HICHER P.-Y., *An elastoplastic model for granular materials with microstructural consideration*, Int. J. of Solids and Structures, 2005, Vol. 42, No. 14, 4258–4277.

[7] CHUPIN O., SAIYOURI N., HICHER P.-Y., *Numerical modelling of cement grout in saturated porous media*, 16th ASCE Engineering Mechanics Conference, Seattle, 2003.

[8] CHUPIN O., SAIYOURI N., HICHER P.-Y., *Tthe effects of filtration on the injection of cement-based grouts in sand columns*, Transport in Porous Media (accepted for publication).

[9] CLOUGH G.W., SITAR B., *Cemented sand under static loading*, Journal of the Geotechnical Engineering, 1981, 107(GT6), 799–817.

[10] DANO C., *Comportement mécanique des sols injectés*, PhD thesis Université de Nantes et Ecole Centrale de Nantes, 2001.

[11] DANO C., HICHER P.-Y., *Behavior of uncemented soils and grouted soils before maximum shear strength*, Soils and Foundations, 2003, 43, No. 4, 13–20.

[12] DANO C., HICHER P.-Y., TAILLIEZ S., *Engineering properties of grouted sands*, Journal of Geotechnical and Environmental Engineering, ASCE, 2004, Vol. 130, No. 3, 328–338.

[13] DUPAS J.M., PECKER A., *Static and dynamic properties of sand-cement*, Journal of the Geotechnical Engineering Division, Proceedings of the American Society of Engineers, 1979, 105(3), 419–436.

[14] LIAO C.L., CHANG T.P., YOUNG D., CHANG C.S., *Stress–strain relationship for granular materials based on hypothesis of best fit*, International Journal of Solids and Structures, 1997, 34 (31–32), 4087–4100.

[15] MAALEJ Y., *Comportement mécanique d'un milieu granulaire injecté par un coulis de ciment: étude expérimentale et modélisation micromécanique*, PhD thesis, Ecole Nationale des Ponts et Chaussées, 2007.

[16] MINDLIN R.D., *Microstructure in linear elasticity*, Arch. Rational Mech. Anal., 1969, 16, 51–78.

[17] ZEBOVITZ S., KRIZEK R.J., ATMATZIDIS D.K., *Injection of fine sands with very fine cement grout*, Journal of Geotechnical Engineering, 1989, 115, No. 12, 1717–1733.